Wolf-Rayet Stars
W.-R. Hamann, A. Sander, H. Todt, eds.
Potsdam: Univ.-Verlag, 2015
URL: http://nbn-resolving.de/urn:nbn:de:kobv:517-opus4-84268

Modelling colliding wind binaries in 2D

T. Hendrix & R. Keppens
CmPA, Department of Mathematics, KU Leuven, Celestijnenlaan 200B, 3001 Leuven, Belgium

We look at how the dynamics of colliding wind binaries (CWB) can be investigated in 2D, and how several parameters influence the dynamics of the small scale structures inside the colliding wind and the shocked regions, as well as in how the dynamics influence the shape of the collision region at large distances. The parameters we adopt are based on the binary system WR98a, one of the few Wolf-Rayet (WR) dusty pinwheels known.

1 Physical setup

We model the binary system WR98a based on the information available from current observations. The system was identified to contain a WC8 or WC9 star (Williams 1995). Monnier (1999) revealed that WR98a forms a "pinwheel nebula" in infrared, suggesting an OB type companion. We model the WR star as a WC9 subtype and use a mass of $M_{\rm WR} = 10M_\odot$ (Sander 2012), mass-loss rate $\dot{M}_{\rm WR} = 0.5 \times 10^{-5}$ M$_\odot$ yr^{-1} (Monnier 2002), and wind velocity $v_{\infty,\rm WR} = 900$ km s^{-1} (Williams 1995). The OB type companion is less constrained. We assume $M_{\rm OB} = 18M_\odot$, $\dot{M}_{\rm OB} = 0.5 \times 10^{-7}$ M$_\odot$ yr^{-1}, and $v_{\infty,\rm OB} = 2000$ km s^{-1}. The momentum flux ratio of the winds is then $\eta = \dot{M}_{\rm OB} v_{\infty,\rm OB} / \dot{M}_{\rm WR} v_{\infty,\rm WR} = 2.22 \times 10^{-2}$, thus the WR outflow dominates. With an orbital period of 565 days (Williams 2003), the semi-major axis length of the orbit is $a = 6.08 \times 10^{13}$ cm.

2 Numerical setup

Following the methodology we employed in Hendrix & Keppens (2014) and Hendrix (2015), we use the gas+dust hydrodynamics module of the `MPI-AMRVAC` code. The dynamics is described by using the coupled gas+dust fluid equations (see Hendrix & Keppens 2014; Porth 2014). Additionally, optically thin radiative cooling of the gas fluid is taken into account in several simulations as an additional term to the energy equation (van Marle & Keppens 2011). In the outflow of WR stars the high metallicity strongly enhances the radiative cooling. We use an adequately adapted table by Mellema & Lundqvist (2002). The physical domain between x,$y \in$ [-160a,160a] is simulated on a Cartesian grid with an effective resolution of 81920×81920 by using 11 adaptive mesh refinement (AMR) levels. The winds are introduced through boundaries at the terminal radii (5×10^{12} cm and 3×10^{12} cm for the WR and OB star, respectively). The stars follow their (counter-clockwise) Keplerian orbit. We use two tracer fluids that are advected with the flow to separately track the material ejected by the stars. The mixing of WR and OB material can be quantified by the product of the tracers.

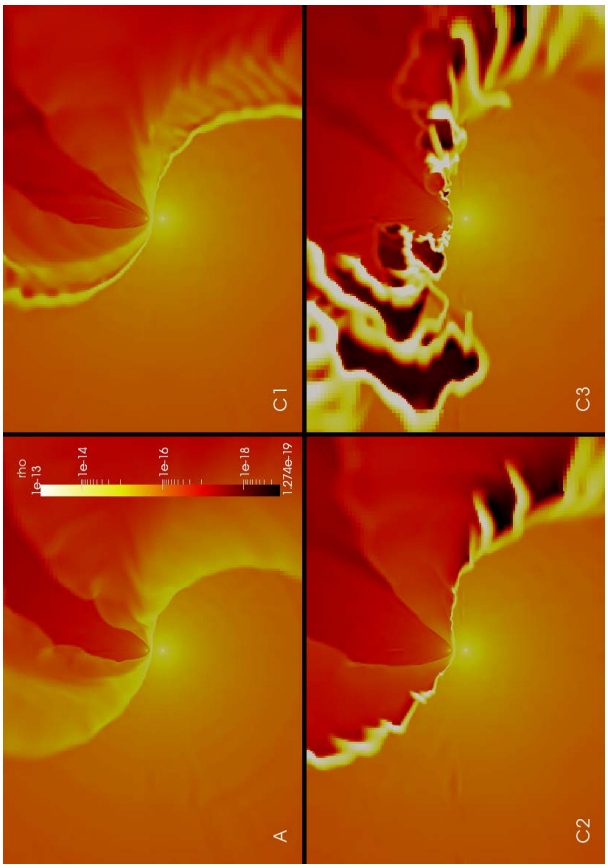

Fig. 1: Densities in A and 3 versions of C with reduced cooling at $t = 0.25$. The region shown is the central (8×10^{14} cm) × (5.6×10^{14} cm).

3 (Ir)relevance of 2D simulations

A model of a colliding wind binary can be seen to be inherently 3D due to the orbital motion of two stars and the non-axisymmetric interaction of the stellar winds. Nevertheless, the question can be asked to which degree it would be useful to consider a similar model in 2D. Due to the non-axisymmetric features the model is preferentially evaluated in a Cartesian grid. This however means that the outflow, for which the density in our model is calibrated at the terminal velocity radius, is no longer physically representative in 2D. In practice this means that density and

pressure patterns may not correspond to the structures in 3D. For colliding wind binary simulations this specifically has influence on the density structures (and contrasts). Radiative cooling is strongly influenced in these cases. 3D simulations will be discussed in Hendrix et al. (2015), however when compared to 2D simulations we see that radiative cooling produces great differences in the obtained results. Nevertheless, 2D simulations are less demanding, and therefore many dynamical simulations of WR (and other) binaries are performed in 2D. Typically, to obtain results that are more comparable to full 3D setups, η is altered so that $\eta_{2D} = \sqrt{\eta_{3D}}$. In this way, the contact discontinuity (CD) of the wind collision shock is located at the same distance between the stars in 2D as in 3D. While this is typically done to obtain a shock location and structure resembling the 3D situation (close to the wind collision region (WCR)), the actual physical correctness of the values is given up. In the following we use 2D simulations to investigate the importance of several parameters on the formation of structures in the WCR and the subsequent outflow. Table 1 gives an overview of the parameters used.

Tab. 1: Parameters in the simulations: the adiabatic index γ, the ellipticity of the orbit (ϵ), the physical domain size (x and y axis length), radiative cooling (C) or not (NC), and the number of AMR levels. Model C represents 3 simulations with altered cooling.

	A	B	C	D	E
γ	5/3	4/3	5/3	4/3	5/3
ϵ	zero	zero	zero	0.7	zero
Domain	$320a$	$320a$	$320a$	$1280a$	$1280a$
Cooling	NC	NC	C	NC	NC
levels	11	11	11	13	13

3.1 Radiative cooling

In 2D, partly due to the switching from η to $\sqrt{\eta}$, densities are typically higher, and therefore the effect of radiative cooling is strongly enhanced. This results in spurious instabilities, something which may not be seen in 3D. To obtain shock structures comparable to those in 3D and to investigate the effect of radiative cooling, we artificially lower the cooling rate to a factor ω. Figure 1 gives a comparison at $t = 0.25$ between setup A and the different cases of C with ω=0.01, 0.05, and 0.2. When going from no cooling to the weakest cooling, ω=0.01, we see that the cooling compresses the region between the WR-shock and the CD. Also, instabilities cause this region (specifically on the trailing arm) to collapse in dense ripples with lower density regions in between. When cooling is further enhanced ($\omega = 0.05$, case C2) the WR-shock and the CD have fully collapsed and produce a compressed region with significantly enhanced densities. Ripples can be seen to form barbed structures in both the trailing and leading shock, however the effect is stronger in the trailing arm where an alternating high and low density pattern forms. The density ratio in these regions is as strong as 5–6 orders of magnitude. For even higher cooling ($\omega = 0.2$, case C3) the instabilities are even further enhanced. The high density structures form a broad region as they move out due to random unstable motions when the thermal instability takes place. If we would increase cooling even further, the motion of the thermal unstable wind collision zone can become so violent that the shock region temporarily or continuously starts to move between (and over) the two stars. Such movement may result in strong mass removal from the stellar surface.

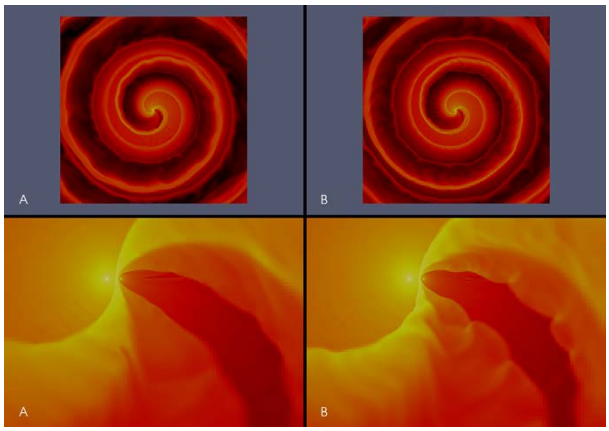

Fig. 2: Densities in A and B at $t = 3.0$, using the same colour scale as figure 1. The top figures show the full domain, the bottom figures are zoomed in near the binary.

A 3D setup of C with $\omega = 1.0$ results in structures in between C2 and C3. The effect of cooling on the dynamics and structure formation in CWB is found to be of great importance to realistically model the WCR in CWB. Local density enhancements due to thermal instabilities are of great importance towards obtaining dust formation. While typical WR wind conditions are unlikely to form significant amounts of dust, density enhancements due to shocks and radiative cooling enhance the formation rate.

3.2 The adiabatic index γ

We are interested to see if a change from $\gamma = 5/3$ (typically assumed in similar setups) to $\gamma = 4/3$ influences the structure formation and mimics some of the effects typically associated with radiative cooling. Figure 2 compares setups A and B at $t = 3.0$. Results can be seen to be similar. The large scale structures and densities in the spirals are nearly identical. If we look at the inner WCR (shown in the bottom panels of figure 2) we see that B with

$\gamma = 4/3$ is slightly more unstable, producing "knots" on the OB-shock and high densities ripples on the CD. While the rippling instabilities B are similar as to cases with weak cooling ($\omega = 0.01$ in section 3.1), the effect is less strong. The ripples of the CD produces visible patterns on the large scale, however their effect on the large scale evolution is small.

3.3 Ellipticity

In the simulation D with elliptic orbit, the periastron passage occurs when the OB star is left of the WR star in the images. While the ellipticity in simulation D is significant at $\epsilon = 0.7$, except for being slightly lopsided, few important differences are seen between setups D and E. While average densities are higher on the periastron side than the apastron side, the density range is similar and no additional high density structures are formed. The density asymmetry is an effect of the orbital velocity of the OB star. This pattern has previously been predicted by the dynamical model of Parkin & Pittard (2008), however only the location of the CD is calculated in their model. A combination of cooling with ellipticity may potentially introduce stronger differences as the effectiveness of the thermal instability may vary based on orbital phase.

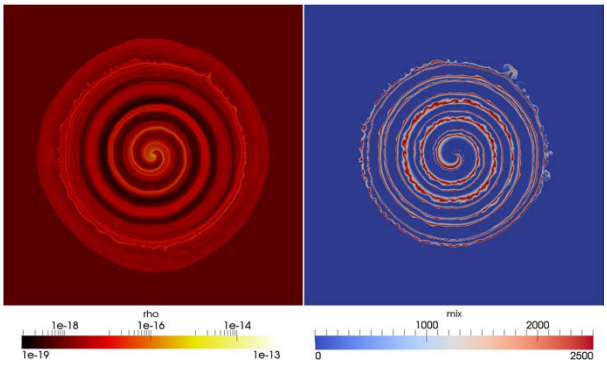

Fig. 3: Density profile (left) and the mixing (right) in E at $t = 6.3$. The entire physical domain is shown.

3.4 Mixing and large scale structures

The mixing zones, shown on large scale in figure 3 and closer to the binary in figure 4, are located around the CD. On the leading edge mixing is closely bound to the CD, while on the trailing edge a broad mixing layer is seen. High velocity and low density material is injected by the OB star. It is confined between the two CDs, causing the low density spiral pattern in figure 3. Because of the velocity shear between the two wind regions the CD is prone to Kelvin-Helmholtz instabilities (KHI). The wind motion is mostly radial. The transverse velocity $\vec{v} - (\vec{v} \cdot \hat{r})\hat{r}$ is parallel to the spiral pattern at larger distances. Interestingly the confined OB material has a much stronger transverse component: while 98% of the velocity of the WR wind is radial, this is only 75–87% for the OB wind. Furthermore, the confined OB material has a significant transverse velocity difference with the surrounding material, which causes shearing along the CD. After one spiral winding the mixing layer along the trailing CD begins to show the onset of a KHI. Nevertheless, on larger scale we see that the spiral stays stable. This extends the findings of Lamberts (2012), who found that a comparable setup was stable in their smaller domain.

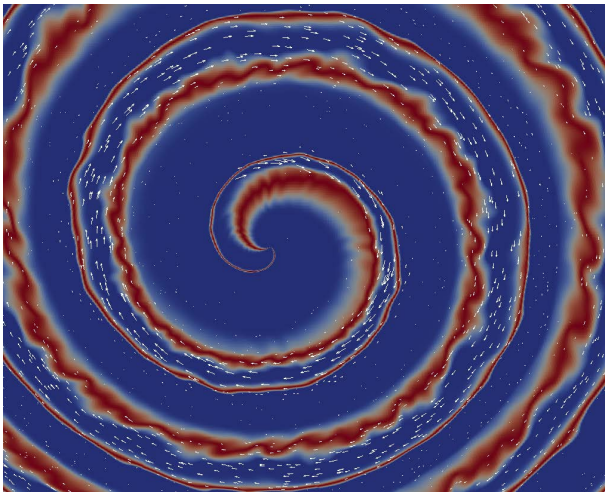

Fig. 4: Mixing in the central region of E at $t = 6.75$. The colour scale is the same as in figure 3.

References

Hendrix, T. & Keppens, R. 2014, A&A, 562, A114
Hendrix, T., van Marle, A. J., Keppens, R., Camps, P., & Meliani, Z. 2015, in preparation
Hendrix, T. e. a. 2015, A&A, 575, A110
Lamberts, A. e. a. 2012, A&A, 546, A60
Mellema, G. & Lundqvist, P. 2002, A&A, 394, 901
Monnier, J. D. e. a. 1999, ApJ, 525, L97
Monnier, J. D. e. a. 2002, ApJ, 566, 399
Parkin, E. R. & Pittard, J. M. 2008, MNRAS, 388, 1047
Porth, O. e. a. 2014, ApJS, 214, 4
Sander, A. e. a. 2012, A&A, 540, A144
van Marle, A. J. & Keppens, R. 2011, Computers and Fluids, 42, 44
Williams, P. M. e. a. 1995, MNRAS, 275, 889
Williams, P. M. e. a. 2003, in IAU Symposium, Vol. 212, , 115

Andy Pollock: Is the hot shocked gas also formed here encased by the dust spiral which might account for the absence of observed X-rays from many of these systems?

Tom Hendrix: No, I don't think that is the case in general, as the X-ray source is probably located in between the stars in the wind collision region, while dust is formed much further away in the interaction region (at 20 AU from the stars in these simulations).

Jesús A. Toalá: Why do you have the dust-emission zone coincident with the lowest density region? It seems weird for me!

Tom Hendrix: We see that the dust is formed in the inner wind collision region at the contact discontinuity (CD) where material from the two stars is being mixed. In this region the densities are high. However, at larger distances (further out than the outer dust forming limit), these regions are perturbed by instabilities. The dust, which was formed at the CD surrounding the low-density region, is then transported and mixed into the low-density region at larger distances. Hence, the presence of the dust in the low-density region is a result of dynamics, and the dust is not formed in the low-density region.

Jose Groh: If I understood correctly, your plan is to do post-processing radiative transfer using the output of the hydrodynamic simulations. But wouldn't you expect feedback effects from the dust onto the hydrodynamics?

Tom Hendrix: Yes! The dust, which is dynamically taken into account as an additional fluid in these simulation, influences the dynamics of the system, certainly when the dust-to-gas mass density ratios are as high as observed here (up to 0.33). In a recent paper (Hendrix & Keppens 2014, A&A, 562, A114) we demonstrated that dust can stabilise the Kelvin-Helmholtz instability (KHI) under certain conditions, and that the KHI strongly influences the density distribution of dust. We have not yet investigated the effect of dust on the other instabilities seen in the setup in full detail (thin-shell instability, Rayleigh-Taylor instability, and Richtmyer-Meshkov), but also there an effect on the dynamics can be expected depending on the setup.